This is the post print version of the article, which has been published in Journal of tissue engineering and regenerative medicine 2017, 11 (10), 2752-2762. http://doi.org/10.1002/term.2170.

Differentiation of adipose stem cells seeded towards annulus fibrosus cells on a designed poly(trimethylene carbonate) scaffold prepared by stereolithography

Sébastien B.G. Blanquer [a,d,1], Arjen W.H. Gebraad [a,1], Susanna Miettinen [b], André A. Poot [a,d], Dirk W. Grijpma[a,c,d], Suvi P. Haimi [a,e*]

[a] MIRA Institute for Biomedical Technology and Technical Medicine, Department of Biomaterials Science and Technology, University of Twente, Enschede, The Netherlands.

[b] Institute of Biosciences and Medical Technology (BioMediTech), University of Tampere, Tampere, Finland.

[c] University of Groningen, University Medical Center Groningen, W.J. Kolff Institute, Department of Biomedical Engineering, Groningen, The Netherlands.

[d] Collaborative Research Partner Annulus Fibrosus Rupture Program of AO Foundation, Davos, Switzerland.

[e] Department of Oral and Maxillofacial Sciences, Clinicum, University of Helsinki Helsinki, Finland.

[1] These authors contributed equally to this work.

* Corresponding author.
Dr. Suvi P. Haimi
Department of Oral and Maxillofacial Sciences, Clinicum
Faculty of Medicine, PO Box 41, 00014
University of Helsinki
Finland
Tel: + 358 44 0291203
Email: suvi.haimi@helsinki.fi

1. Introduction

The annulus fibrosus (AF) is a multi-lamellar fibrocartilaginous tissue which forms the outer layer of the intervertebral disc (IVD) and is subjected to high risk of degeneration due to its avascularity and low cellularity (Bibby *et al.* 2001). Degeneration of the IVD leads to tearing of the AF (Coppes *et al.* 1990). Already even minor injuries to the AF can lead to permanent disc damage (Fazzalari *et al.* 2001). The conventional treatments by drug administration (Blanquer *et al.* 2015) and/or the established surgical methods have shown serious drawbacks and limited success (Bao *et al.* 1996, Disch *et al.* 2008). Therefore, new effective treatments are urgently needed. Tissue engineering of AF is a promising approach allowing immediate closure of the defect, restoring the biomechanical properties of the disc and simultaneously encouraging the repair of the ruptured tissue.

Several scaffold processing techniques with different types of biodegradable biomaterials have been suggested for AF tissue engineering (Guterl *et al.* 2013). Unfortunately, none of the current strategies have been able to reach the biomechanical properties of the native AF tissue and restore its function. A major challenge has been the reproduction of the complex multi-lamellar structure and the biomechanical cues of the native tissue (Figure 1 A and 1B) (Ebara *et al.* 1996, Nerurkar *et al.* 2010), which are prerequisites for efficient cell differentiation and extracellular matrix (ECM) organization (Guterl *et al.* 2013). Therefore, a scaffold for AF regeneration must preferably induce the specific orientation and direction of the collagen bundles. An accurately-controlled 3D scaffold preparation method that is able to reproduce the complex organization and orientation of the pore characteristics of the damaged tissue, has not yet been reported. Stereolithography could be used to create these complex designs as it is known to be a most versatile 3D structure processing method, with the highest accuracy and precision (Melchels *et al.* 2010, Skoog *et al.* 2014) of the additive manufacturing techniques.

In addition to the scaffold design and preparation challenge, a suitable cell source and efficient differentiation method need to be available for a successful cell therapy leading to functional AF matrix synthesis and disc regeneration. Although autologous AF cell transplantation therapies have encountered some success in animal models (Kuh *et al.* 2009), an alternative for clinical therapy is ineluctably required due to the limited availability and expansion capacity of autologous AF cells (Bron *et al.* 2009). Bone marrow-

derived mesenchymal stem cells (BMSCs) have been used for AF tissue engineering applications (Richardson *et al.* 2010, Orozco *et al.* 2011). However, the use of these cells is also limited by the quantity that can be collected from the patient, and by the associated donor-site morbidity. The use of multipotent human adipose stem cells (hASCs) differentiated towards an AF phenotype could evade these problems as adipose tissue is an abundant and easily accessible cell source (Lindroos *et al.* 2011). Interestingly, recent studies have shown that isoforms of TGF-β can stimulate the differentiation of animal and human derived ASCs towards an AF phenotype (Tapp *et al.* 2008, Gruber *et al.* 2010). However, a systematic comparison between the key isoforms of TGF-β, type 1 and 3, and their use in combination to efficiently differentiate hASCs towards an AF phenotype is lacking.

In this work we aim to establish an effective method to engineer AF tissue using novel AF-mimetic designed scaffolds seeded with hASCs and differentiated *in vitro* under optimized culture conditions. This is the first study describing the preparation of a tissue engineering scaffold with a pore architecture representing the orientation of the collagen bundles of the AF tissue. Because both mechanical properties and the architecture of the scaffold play an important role in the biological response, we propose to use resins based on poly(trimethylene carbonate) (PTMC). This polymer is known for its biocompatibility and biodegradability (Zhang *et al.* 2006, Vyner *et al.* 2014) but also for its rubber-like properties (Schuller-Ravoo *et al.* 2013). To allow effective hASC differentiation towards AF tissue, a new hASC differentiation strategy was established, based on optimization of seeding method and TGF-β1 and -3 isoform supplementation.

2. Materials and methods

2.1 Scaffold fabrication and characterization

The scaffolds were designed using 3D software (Rhinoceros 3D, McNeel Europe and K3dSurf v0.6.2).

The synthesis of PTMC oligomers (Mn = 5000 g/mol) was carried out by ring-opening polymerization of 0.98 mol (100 g) trimethylene carbonate (1,3-dioxan-2-one; TMC, Foryou Medical, Huizhou City, China), initiated by 0.0196 mol (2.62 g) tri(hydroxymethyl)propane (TMP, Sigma-Aldrich, Munich, Germany) and catalyzed by

0.05 wt% stannous octoate (tin 2-ethylhexanoate, SnOct2, Sigma-Aldrich) at a temperature around 130°C for 3 days under argon atmosphere. Subsequently, the oligomer was end-functionalized with methacrylate groups using 0.18 mol (27 mL) of methacrylic anhydride in the presence of 0.18 mol (25 mL) of triethylamine in solution in dichloromethane (100 mL) (Sigma-Aldrich) at room temperature under argon atmosphere for 5 days.

Proton nuclear magnetic resonance (1H-NMR, 300 MHz) was used to determine the conversion rate and the number average molecular weight (Mn) of the macromer. The resin for stereolithography was prepared by dilution of the PTMC macromer in propylene carbonate (Sigma-Aldrich) to reach a viscosity of approximately 5-10 Pa.s. The resin further contained Lucirin TPO-L (5 wt% relative to the macromer) (BASF, Germany) as a photo-initiator and Orasol Orange dye (0.15 wt% relative to the macromer) (Ciba Speciality Chemicals, Switzerland) to control the penetration depth of the UV light. The scaffolds were built using a UV stereolithograph (EnvisionTech Perfactory, Germany) at a pixel resolution 16x16 μm^2 and a layer thickness of 100 μm per layer. To reach this resolution with this resin composition, the illumination time per layer was 20 seconds with a light intensity of 180 mW/cm^2. After extraction twice for 6 hours in acetone (Sigma-Aldrich), the scaffolds were washed with 70% ethanol (Sigma-Aldrich) for 6 more hours and dried until a constant weight was reached.

The mechanical properties of the scaffolds were measured by compression testing in the dry state using a material testing machine (Zwick Z020, Germany), equipped with a 500N load cell at a compression rate of 30% per minute to a maximum of 80% strain.

Scanning electron microscopy (SEM) (Philips XL30 ESEM-FEG, The Netherlands) was applied to visualize the porous structures. The specimens were sputter-coated with gold, and the apparatus was operated at a voltage of 3 kV.

2.2 Adipose stem cell isolation and characterization

Human ASCs were isolated from 6 female donors (age 52±9) and expanded in maintenance medium (MM; Table 1) at 37°C and 5% carbon dioxide (CO_2) as previously described (Kyllonen *et al.* 2013). The study was carried out under approval of the ethical committee of Pirkanmaa Hospital District and with informed consent from the donors.

After expansion, hASCs were characterized by flow cytometry (FACSAria; BD Biosciences, Belgium) to confirm the mesenchymal origin of the cells. Monoclonal

antibodies against CD14-PE-Cy7, CD19-PE-Cy7, CD45RO-APC, CD73-PE and CD90-APC (BD Biosciences); HLA-DR-PE (Immunotools GmbH, Germany) and CD11a-APC, CD80-PE, CD86–PE, and CD105-PE (R&D Systems Inc, USA) were used. Analysis was performed on 10,000 cells per samples and positive expression was defined as the level of fluorescence greater than 99% of the corresponding unstained cell sample.

2.3 Differentiation medium component optimization in micromass cultures

To optimize the AF differentiation medium for hASCs, a preliminary screening of the potential growth factors was done in a micromass culture. For this, hASCs at passages 3-4, were plated according to the micromass culture technique described earlier (Tapp *et al.* 2008) in order to stimulate AF differentiation. A high cell density suspension (10^7 cells/ml) was added as 3 droplets of 10 µl to the centre of wells in 24-well plates (Nunc). Cultures were incubated for 3 h before addition of 700 µl control chondrogenic medium (CM), or differentiation media consisting of CM supplemented with either 10 ng/ml TGF-β1 (DM1), 10 ng/ml TGF-β3 (DM3) or both 10 ng/ml TGF-β1 and 10 ng/ml TGF-β3 (DM1+3) (Table 1). A concentration of 10 ng/ml was used as this concentration for both TGF-β1 and TGF-β3 has been shown previously to be effective for hASCs (Gruber *et al.* 2010). Experiments were repeated 3 times with different donors. Technical duplicates of each sample were used in all assays. After 14 and 21 days of culture, the micromasses were collected for biochemical, histological and PCR analysis. DM3 was selected as AF differentiation medium for the subsequent scaffold experiments based on the obtained results (see section 2.1).

2.4 Adipose stem cell seeding in scaffolds

The scaffolds were pre-treated with CM 24 h prior to cell seeding. At passages 3-4, hASCs were seeded in the scaffolds using micromass, fibrin or direct seeding. In the micromass seeding group, hASCs were suspended in MM at high cell density (10^7 cells/ml) as described in section 1.3, and 2 cell suspension droplets of 10 µl were carefully applied to the lateral sides of the scaffold. In the fibrin seeding group, 180,000 hASCs were suspended in 20 µl of fibrinogen solution (33.3 mg/ml) and then combined with 20 µl of thrombin solution (1 U/ml) immediately before pipetting into the scaffold (Baxter Biosurgery, Vienna, Austria). In the direct seeding group, 180 000 hASCs were suspended in 40 µl of

MM and pipetted directly into the scaffold. It should be noted that in the direct and fibrin seeding, the initial cell number was 10% lower than compared to micromass seeding. The maximum number of cells that could be kept in suspension in a 40 µl volume was 180 000. A single cell suspension is critical for direct seeding. The cell-seeded scaffolds were incubated at 37°C and 5% CO_2 for 3 h (micromass and direct seeding groups) to allow cell attachment or for 1 h (fibrin seeding group) to allow fibrin gelation before transferring the scaffolds to new wells in 24-well plates (Nunc) with 1 ml of DM3. Scaffolds with pure fibrin gel without hASCs were used as blanks in all the assays to take into account the background caused by the fibrin gel in the assays. In the direct- and micromass seeding groups, scaffolds without fibrin and without hASCs were used as blanks. Experiments were repeated 3 times with different donors. Technical duplicates of each sample were used in all assays. After 1, 14 and 21 days of culture, the cell-seeded scaffolds were collected for biochemical, histological and PCR analysis.

2.5 Annulus fibrosus cell culture in scaffolds

In order to verify the phenotype of the differentiated hASCs towards AF tissue we used human AF cells (ScienCell Research Laboratories, Carlsbad, CA, USA) seeded with fibrin gel (human AF cells; ScienCell Research Laboratories, Carlsbad, CA, USA) as a reference cell type. Fibrin gel-seeded AF cells have been previously shown to maintain the typical features of these cell populations (Colombini *et al.* 2014). Human AF cells were expanded according to the manufacturer's protocol in a commercially available medium (NPCM; ScienCell) at 37°C, 5% CO_2. After expansion, cells of passage 4 were seeded into the scaffolds using fibrin gel seeding as described in detail in section 1.4. After 2 and 3 weeks of culture, scaffolds were collected for biochemical and PCR analysis.

2.6 Biochemical analysis of the micromass cultures and the cell-seeded scaffolds

For biochemical analysis, micromass cultures were digested for 48 hours with 1.25 U/ml papain (Sigma-Aldrich) at pH 6.5 and 65 ^{o}C. Cell-seeded scaffolds were rinsed with PBS and digested overnight under identical conditions. The amount of DNA in the micromass culture lysates was quantified using 0.2 µg/ml Hoechst 33258 nucleic acid stain (Bio-Rad Laboratories Inc., Hercules, CA, USA) with purified calf thymus DNA as a standard (Bio-Rad). Fluorescence was measured with a multiplate reader (Victor 1420 Multilabel Counter;

Wallac, Turku, Finland) using excitation at 360 nm and emission at 460 nm. The amount of DNA in the cell-seeded scaffold lysates was evaluated by using the CyQuant proliferation assay (Invitrogen, Carlsbad, CA, USA) as previously described by our group (Haimi *et al.* 2009a). A standard curve was prepared by serial dilution of bacteriophage λ DNA (Invitrogen). Fluorescence (excitation at 480 nm, emission at 520 nm) was measured using a microplate reader (Infinite 200 PRO series, Tecan, Männedorf, Switzerland).

The total amount of sulphated glycosaminoglycans (sGAG) in the papain lysates of the micromass cultures and the cell-seeded scaffolds was analysed with a sGAG assay kit (Blyscan, Biocolor Ltd, Carrickfergus, UK) according to manufacturer's instructions. A standard from the kit consisting of chondroitin 4-sulphate sodium salt from bovine trachea was used in order to quantify the total amount of sGAG. Absorbance was measured at 656 nm in the multiplate reader (Victor).

Total collagen content of the cell-seeded scaffolds was quantified using a hydroxyproline assay (Sigma-Aldrich). The papain lysate was hydrolysed in 6N hydrochloric acid solution (Sigma-Aldrich) at 110°C for 3 hours followed by quantification of hydroxyproline content based on the reaction of oxidized hydroxyproline with 4-(dimethylamino)benzaldehyde (DMAB). Absorbance was measured at 544 nm in the multiplate reader (Victor). Collagen content was calculated based on the reported weight ratio of hydroxyproline:collagen of 0.125 (Edwards and Obrien 1980), assuming that elastin content was negligible.

2.7 Histological staining

Micromass cultures were fixed for 1 h in 4% paraformaldehyde (Sigma-Aldrich), embedded in paraffin and sectioned at 5 µm thickness for histological analysis. Proteoglycan production in the ECM was assessed by toluidine blue staining (0.1% vol in dH2O; Sigma-Aldrich) (Tapp *et al.* 2008).

Cell attachment and distribution in the scaffolds was evaluated using methylene blue staining. Prior to methylene blue (Sigma-Aldrich) staining, the scaffolds were fixed in 4% paraformaldehyde solution. After fixation, cells were stained with methylene blue solution (1 % in borax (B-3545 Borax (99.5-105 %), Sigma Aldrich) and rinsed with PBS to eliminate the excess of methylene blue. Subsequently, cell attachment and distribution in the scaffold was assessed using a stereomicroscope (Nikon SMZ-10A with Sony 3CCD camera).

To evaluate collagen deposition, the cell-seeded scaffolds were fixed in 4% paraformaldehyde solution, transferred to 5% sucrose (Sigma-Aldrich) overnight, embedded in Jung tissue freezing medium (Leica Microsystems, Germany) and frozen at -20 ^{o}C. Subsequently, the scaffolds were sectioned at 14 µm thickness using a Shandon cryotome (Cryostat series Shandon, France). The cross-sections were placed on glass slide and then dried for 3 days. The production of collagen in the cell-seeded scaffolds was evaluated by Picrosirius Red (Polysciences kit, PA, USA) staining following the producer's protocol. The microscopic preparations were visualized with a Nikon E600 Fluorescence/Histology microscope (Nikon Cooperation, Tokyo, Japan). Polarized light was used to detect oriented collagen fibres.

2.8 Gene expression of differentiated hASCs and native AF cells

Quantitative reverse transcription polymerase chain reaction (qRT-PCR) was used to study the relative expression of AF phenotype related genes in micromass cultures and in cell seeded scaffolds. Total RNA was isolated using the NucleoSpin® RNA II Total RNA isolation kit (Macherey-Nagel GmbH & Co. KG, Germany) according to the manufacturer's instructions. Total RNA yield was measured by optical density at 260 nm with a Nanodrop 1000 spectrophotometer (Thermo Fisher Scientific, Waltham, MA, USA), and sample purity was assessed from the ratio of A260/A280. The iScript cDNA Synthesis Kit (Bio-

Rad, Hercules, CA, USA) was used to prepare cDNA from the total RNA. Reverse transcription was performed using a Bio-Rad CFX96 Real-Time PCR system.

Gene expressions of aggrecan, decorin, collagen type I and type II were analysed in micromass cultures. Moreover, also collagen type V expression was analysed in the cell-seeded scaffolds. Gene expression was assessed by PCR analysis using human acidic ribosomal phosphoprotein P0 (RPLP0) as a reference gene, which has been shown to be stably expressed under several experimental conditions (Gabrielsson *et al.* 2005, Fink *et al.* 2008). The primer sequences (Sigma-Aldrich) are presented in Table 2.

Reaction mixtures contained a maximum of 50 ng cDNA, 300 nM forward and reverse primers and Power SYBR® Green PCR Master Mix (Applied Biosystems, Foster City, CA, United States). The PCR reactions were conducted in duplicates and monitored using the ABI Prism® 7300 Sequence Detection System (Applied Biosystems) starting with initial activation at 95°C for 10 min, followed by 45 cycles of denaturation at 95°C for 15 s and annealing and extending at 60°C for 60 s. The results were normalized to expression of RPLP0 according to a mathematical model described by Pfaffl (Pfaffl 2001).

2.9 Statistical analysis

Statistical analyses were performed with SPSS version 20 (IBM, Armonk, NY, USA). The effects of medium composition, cell seeding technique and culture duration on DNA content, sulphated GAG content, collagen content and normalized gene expression levels were analyzed using Kruskal-Wallis one-way analysis of variance by ranks, followed by a Mann-Whitney U post hoc test to analyse specific sample pairs for significant differences. The results were considered significant when $p<0.05$.

3. Results

3.1 Structural and mechanical scaffold characterization

A specific truncated cone design was built with a height of 4 mm, a maximum diameter of 4 mm and a minimum diameter of 3 mm. The built scaffolds had a porosity of 76% with an average pore channel diameter of 420 µm (Figure 1C). In order to reproduce the function and the structure of the AF tissue, the pore channels mimic the organization and the orientation of collagen fibres from native AF tissue.

The compression modulus of the cubic designed porous PTMC scaffolds was 0.35±0.10 MPa. This indicates that the scaffolds are flexible, possibly allowing shearing between different lamellae of the native AF (Nerurkar *et al*. 2009). In future work, the mechanical properties of the scaffolds during the whole culture period should be evaluated.

3.2 Adipose stem cell characterization

Human ASCs demonstrated high expression (>85%) of CD90 (Thy-1) and CD105 (endoglin), moderate (>50%) or high expression of CD73 (ecto 5' nucleotidase) and no or low expression (≤2%) of CD11a (lymphocyte function-associated antigen 1), CD14 (monocyte and macrophage marker), CD19 (dendritic cell marker), CD45RO (pan-leukocyte marker), CD80 (B cell marker), CD86 (antigen presenting cell marker), and HLA-DR (HLA class II). The results showed that hASCs expressed most of the specific antigens that define human stem cells of mesenchymal origin according to the Mesenchymal and Tissue Stem Cell Committee of the ISCT (Dominici *et al.* 2006).

3.3 Optimization of differentiation medium components in micromass cultures

The biochemical analyses of the micromasses revealed that the numbers of hASCs were significantly higher at both 14 and 21 day time points in the presence of TGF-β3 (DM3 and DM1+3) as compared to the CM group (Supplementary data Figure 1a). The total cell number did not increase with time in any of the groups. TGF-β3 addition resulted in significantly higher amounts of sulphated GAGs in the DM3 and DM1+3 groups compared to the CM group at 21 days of culture (Supplementary data Figure 1b).

These results were consistent with toluidine blue staining (Supplementary data Figure 1c). Samples cultured in the presence of TGF-β3 had more specific staining of the proteoglycans compared to samples cultured in CM or DM1 at both time points. The highest proteoglycan content was found in samples cultured in DM3 for 14 days. At the 21 day time point, micromasses cultured in CM were notably smaller compared to samples cultured in the presence of TGF-β1 and/or TGF-β3.

The analysis of AF-specific genes in the micromass cultures at 21 days showed the highest aggrecan expressions in hASCs cultured in the presence of TGF-β3 (Supplementary data Figure 1d). However, due to donor variation, no significant differences were found. Consistent with the biochemical analysis and the toluidine blue staining, the addition of

TGF-β1 alone (DM1) or in combination with TGF-β3 (DM1+3) did not significantly increase the aggrecan expression compared to the groups without TGF-β1 (CM and DM3, respectively). The expressions of decorin, collagen type I and type II between the medium groups were not different (data not shown). Based on these results, DM3 was selected for further experiments.

3.4 Methylene blue staining of the seeded scaffolds

Already at day 1, major differences between the different seeding methods were observed as only fibrin gel seeding allowed homogenous methylene blue staining indicating uniform hASC distribution in the scaffolds (Figure 2). The fibrin gel alone did not significantly take up the methylene blue dye as demonstrated in the supplementary information (Supplementary data Figure 2). With micromass- and direct seeding of the cells only few areas were stained by the methylene blue suggesting poor cell attachment attached in the scaffolds. At day 14, the differences were even more pronounced as only with fibrin gel seeding hASCs were homogenously attached throughout the scaffold. Instead, hASCs seeded by micromass seeding were grown in clusters only near the original seeding sites. Direct seeding led to poor distribution of hASCs during the 14 day culture period.

3.5 Biochemical analysis of the seeded scaffolds

Consistent with the results of methylene blue staining, direct seeding in the scaffolds showed significantly lower cell seeding efficiency and proliferation of hASCs compared to the other seeding methods at all measured time points (Figure 3a). Cell numbers at 14 and 21 days were the highest using fibrin gel seeding, the difference being significant compared to direct seeding at all-time points. Furthermore, cell numbers increased significantly with time in the case of fibrin seeding ($p<0.05$), while no increase in cell numbers was observed with micromass and direct seeding. Based on the DNA quantification and methylene blue results we excluded direct seeding from further analysis.

Sulphated GAG and collagen assays were implemented in order to quantify the ECM production of hASCs seeded by fibrin gel or micromass techniques (Figures 3b and c). At 14 days, the collagen production was significantly induced by fibrin seeding while the difference in sGAG production between the two seeding methods was not significant. The superiority of the fibrin seeding method was evident at 21 days as fibrin seeding

significantly enhanced both the sulphated GAG and collagen production of hASCs compared to micromass seeding. The collagen production increased significantly with time in the case of fibrin seeding ($p<0.05$), while the collagen content of micromass-seeded hASCs decreased significantly during the culture period ($p<0.05$).

The sGAG/hydroxyproline ratio was used to determine whether the composition of the produced ECM of differentiated hASCs was similar compared to that of AF cells and native AF tissue (Mwale *et al.* 2004). At both time points, the sGAG/hydroxyproline ratio was similar for hASCs and AF cells, both seeded with fibrin (Figure 3d). Interestingly, the sGAG/hydroxyproline ratio increased significantly with time in the case of micromass-seeded hASCs. At day 21, the sGAG/hydroxyproline ratio for micromass-seeded hASCs was significantly higher compared to that of fibrin gel-seeded hASCs and AF cells.

3.6 Histological evaluation of scaffolds seeded with hASC

Picrosirius red staining of the produced collagen matrix in the scaffolds was in accordance with the quantification of total collagen content (Figures 4 and 3C). Only fibrin-seeded hASCs showed abundant deposition of collagen inside the pore channels (Figure 4B). Importantly, polarized light showed the formation and alignment of collagen fibres in this condition (Figure 4F). In contrast, scaffolds seeded with hASCs using the micromass seeding method (Figure 4C) and the AF cell control (Figure 4D) showed only weak collagen formation and no collagen fibres were detected using polarized light (Figures 4G and 4H).

3.7 Gene expression of differentiated hASCs and native AF cells in the scaffolds

All samples showed expression of aggrecan, decorin, collagen type I, type II and type V at 14 and 21 days of culture in hASC and AF cell-seeded scaffolds (Figure 5). No statistical differences between the gene expression profiles of fibrin gel-seeded hASCs and native human AF cells were found. Especially decorin and collagen type II were expressed similarly in fibrin gel-seeded hASCs and AF cells. On the contrary, aggrecan, collagen type I and type II gene expressions of micromass-seeded hASCs were significantly higher as compared to the expressions of the AF cells at both time points.

4. Discussion

At present, effective treatment strategies to regenerate and repair ruptured AF tissue do not exist. Therefore, there is an unmet clinical need for an effective cell-based strategy to restore the biological and biomechanical functions of degenerated AF tissue. Harvested AF cells from the disc have been studied as a cell source for AF engineering (Gruber *et al.* 2009). However, the use of AF cells has encountered major challenges due to the extremely limited availability of the cells in addition to senescence and decreased or altered ECM production (Gruber *et al.* 2007). Transplantation of hASCs differentiated towards AF-like cells is therefore an attractive alternative. This is the first study describing an efficient approach to engineer AF tissue *in vitro* using fibrin gel seeding and differentiation of hASCs stimulated by TGF-β3 in AF-mimetic PTMC scaffolds.

Due to the high biological and functional complexity of AF tissue structure, scaffolds for AF tissue engineering require precise and sophisticated geometries. Our results show that the combination of fibrin seeded hASCs and the scaffold architecture play a significant role in appropriate AF-like matrix production and collagen alignment. This is in agreement with a previous study showing that collagen orientation is controlled by large-scale microstructures in a scaffold for vascular tissue engineering (Engelmayr *et al.* 2006). Likewise, de Mulder et al. used thermal induced phase separation to prepare a scaffold for meniscus repair, in which collagen fibres were oriented through the channel-like pore architecture of the scaffold (de Mulder *et al.* 2013). However, this technique does not allow a sufficient control of the pore architecture, which is essential to reach the optimal reproduction of the AF tissue structure and function. In consequence, a 3D scaffold with specific micro-architecture able to mimic with high precision the complex architecture of native AF will allow forcing the cells and the produced collagen to follow the porous orientation and therefore reproduce the desired structure and function.

AF tissue is composed of 15-25 loosely connected concentric lamellae consisting of highly organized collagen fibers (Marchand and Ahmed 1990). In the lamella, collagen fibers run parallel and are oriented at an angle-ply of 30°, from the transverse section of the IVD, at the outer side of the AF evolving to 45° at the inner side (Cassidy *et al.* 1989). Each lamella is alternated with another lamella in the opposite direction. Only a few studies have been reported on the development of a scaffold reproducing the complex architecture of the collagen fibers in the AF. Nerurkar et al. reported for the first time an electrospun membrane which replicates the specific angle-ply displayed by the collagen fibers (Nerurkar *et al.*

2009). However, due to limitations of the electrospinning approach, the membrane scaffold was built with only two layers, and cannot be considered as full-sized three-dimensional scaffold. The use of a lamellar silk scaffold has also been reported. However, these approaches cannot be adapted to our purpose, either due to the isotropic random pore structure obtained by the used scaffold preparation process that will influence the biomechanical performance (Park *et al.* 2012), or do not allow the fabrication of a full-sized three-dimensional scaffold that is required to repair a herniated disc (Bhattacharjee *et al.* 2012).

Therefore, none of these previous strategies reported in the literature describe a designed scaffold allowing the precise control of the complex organization and orientation of the collagen bundles from native tissue. This limitation may be the major reason to explain the inability to precisely reproduce oriented collagen fibers in previous works. In consequence, our work presented here is the first study describing a designed 3D scaffold with an oriented channel-like pore architecture reproducing the complex structure of AF tissue. The scaffold design was achieved by precisely respecting the complex and typical multi-lamellar organization and angle-ply of the native AF collagen (illustrated in Figure 1A and B) and built with a high precision by stereolithography. Furthermore, the truncated cone geometry of the scaffold was designed in order to prevent the risk of scaffold extrusion after implantation in the disc defect. This specific geometry allows the use of the scaffold as a plug and increases the stability of the implanted scaffold inside the defect.

To obtain efficient *in vitro* AF differentiation, not only a suitable scaffold design is required but also the differentiation medium for hASCs needs to be defined. Therefore, in the first part of this study we defined a suitable AF differentiation medium for hASCs in 2D culture. The importance of TGF-β1 or TGF-β3 to maintain the AF cell phenotype *in vitro* has been previously reported in several studies (Colombini *et al.* 2014, Guillaume *et al.* 2014). However, to the best of our knowledge this is the first study comparing the effects of TGF-β1 and TGF-β3 or their combination on hASC proliferation and differentiation towards AF tissue. Importantly, all the differentiation experiments in this study were done under serum-free conditions to allow direct application of the results towards clinical therapy. According to the biochemical and histological analysis of the micromass cultures, sGAG and proteoglycan production was substantially enhanced in the presence of TGF-β3 (Supplementary data Figure 1). In addition, the gene expression of aggrecan, which is the

most abundant proteoglycan in AF tissue (Roughley *et al.* 2006), was upregulated in hASCs cultured in the presence of TGF-β3 further evidencing the role of TGF-β3 in promoting hASC differentiation towards AF-like cells. Our results are in line with a recent study where TGF-β3 supplementation stimulated matrix deposition of AF cells in vitro (Guillaume *et al.* 2014). Furthermore, TGF-β3 has been shown to up-regulate aggregan, collagen type I and II gene expression in an in vitro full-organ disc/endplate culture system (Haschtmann *et al.* 2012). Although TGF-β1 has been previously demonstrated to promote cellular proliferation and collagen production of various human cells including AF cells (Jenner *et al.* 2007, Wipff and Hinz 2008, Turner *et al.* 2014), TGF-β1 showed a negligible effect on AF differentiation of hASCs when supplemented alone. Consistently, Hegewald *et al.* showed no significant benefit of TGF-β1 addition in 3D culture of AF cells (Hegewald *et al.* 2014). In our study, the aggrecan expression was the highest when TGF-β1 was used in combination with TGF-β3, however, the difference was not significant. Furthermore, no significant differences were found in the expression of decorin, collagen type I and II between the different medium groups. Since the addition of TGF-β1 to the TGF-β3 supplemented medium did not give a significant benefit, DM3 was considered the most suitable AF differentiation medium for hASCs.

In addition to the composition of the differentiation medium, different cell seeding strategies have been shown to have a major effect on stem cell fate (Ameer *et al.* 2002, Colombini *et al.* 2014). However, an efficient cell seeding strategy that supports mesenchymal stem cell differentiation towards AF tissue has not been previously reported. We therefore wanted to find an efficient cell seeding strategy to stimulate hASC differentiation towards the AF phenotype. Direct seeding was used as a reference method since this approach is traditionally used to seed cells into 3D scaffolds (Haimi *et al.* 2009b), and it has been shown to be suitable for AF cell culture in 3D scaffolds prepared by stereolithography (Blanquer *et al.* 2013). Interestingly, our results showed that hASCs seeded by direct seeding were only poorly attached and spread throughout the scaffolds as compared to micromass and fibrin gel seeding. Moreover, the cell seeding efficiency was extremely low in the case of direct seeding. These results are consistent with a previous study demonstrating major challenges in obtaining a uniform cell distribution in 3D scaffolds using direct cell seeding (Lee *et al.* 2005). Micromass seeding was chosen since it has been used as a standard technique to enhance AF differentiation of ASCs in 3D scaffolds (Tapp *et al.* 2008, Gruber

et al. 2010). Nevertheless, in the latter *in vitro* studies the micromass seeding of hASCs even in the presence of TGF-β3 did not allow a sufficient AF-like matrix production especially in terms of sufficient collagen production. Scaffolds seeded with hydrogels such as hyaluronic acid (Nesti *et al.* 2008) and fibrin (Sha'ban *et al.* 2008) in combination with cells have been suggested to be useful in AF tissue engineering. In order to trigger hASC differentiation towards AF cells, fibrin gel seeding was tested as recent studies demonstrated the importance of fibrin to maintain the typical phenotype of AF cells (Colombini *et al.* 2014) and to promote the production of ECM (Sha'ban *et al.* 2008).

Fibrin seeding of hASC resulted in a significantly enhanced proliferation and AF-like ECM formation, as compared to the other seeding strategies. The higher sGAG content of the fibrin-seeded scaffolds may be explained by a higher retention of synthesized glycosaminoglycans in the fibrin gel as compared to micromass seeding (Ameer *et al.* 2002). Moreover, fibrin seeding resulted in an abundant production of collagen which is the main ECM component of AF tissue (Roughley 2004). Collagen production increased significantly from 14 to 21 days, indicating that the fibrin seeding method together with the designed scaffold fully support the production of collagenous AF-like matrix by the hASCs. Not only the production of sGAG and collagen was significantly upregulated, but the collagen was also organized in a specific manner. Picrosirius red staining of collagen showed that the AF-mimetic architecture of the scaffold led to regularly packed and aligned collagen bundles inside the designed pore channels, which is essential for the biomechanical function of AF tissue (Nerurkar *et al.* 2010). This result is remarkable, as we obtained abundant collagen production and bundle formation in a 3D porous structure under static conditions, without mechanical stimulation. Although the pore characteristics of our scaffold have not yet been optimized, the results obtained in this work do show that collagen bundles can be created and that several collagen bundles appear to be aligned along the pore. This already is considerable progress in the field.

The sGAG to hydroxyproline ratio can be used as a specific parameter to distinguish AF from nucleus pulposus tissue. We found that this ratio was similar for AF cells (approximately 2:1) and differentiated hASCs (approximately 3:1), both seeded with fibrin and cultured for 21 days. These ratios correspond closely to the value reported for native human AF tissue (approximately 2:1) (Mwale *et al.* 2004). In contrast, the sGAG to hydroxyproline ratio for micromass-seeded hASCs was around 57:1, which is significantly

different from the ratios for fibrin gel-seeded hASCs and AF cells, tending towards the ratio reported for nucleus pulposus tissue (26:1) (Mwale *et al.* 2004).

To further verify the obtained AF phenotype, we quantified AF-specific markers on the mRNA level. Aggrecan and decorin are the most overexpressed proteoglycans while collagen type I and II are the major collagens present in the ECM of AF tissue (Roughley *et al.* 2006). However, these collagens are not specific for AF tissue alone. Instead, collagen type V has been shown to be a more specific marker for AF tissue distinguishing AF cells from nucleus pulposus cells and chondrocytes (Clouet *et al.* 2009). In our study, micromass and fibrin-seeded hASCs as well as fibrin-seeded AF cells expressed similar levels of collagen type V. Due to the notable donor variation of the mRNA expression, results were shown as a scatter plot instead of a box plot to demonstrate the response of individual donors (Figure 5). This donor variation is a typical of hASCs and other adult stem cells, as has been described earlier (Chou *et al.* 2011, Bieback *et al.* 2012, Kyllonen *et al.* 2013). Nevertheless, our results show that the AF-related gene expression profiles of fibrin-seeded hASCs and human AF cells were not significantly different. These results together with the sGAG to hydroxyproline ratio of 3:1 indicate the potential of fibrin seeding of hASCs in AF tissue engineering. In contrast, micromass-seeded hASCs differed significantly from the AF cells in terms of aggrecan, collagen type I and collagen type II gene expression.

5. Conclusions

In this study, we demonstrated that stimulation with TGF-β3 induces efficient differentiation of hASCs towards AF-like cells. Furthermore, we evaluated the extracellular matrix production by hASCs seeded in an AF-mimetic PTMC scaffold using direct, fibrin gel or micromass seeding in a defined differentiation medium supplemented with TGF-β3. The designed scaffold was prepared by stereolithography in order to mimic the complex architecture of native AF tissue in terms of collagen fiber organization and orientation. Fibrin gel seeding allowed more uniform cell attachment and spreading in the scaffold, as compared to the other seeding methods. Importantly, fibrin seeding significantly stimulated sGAG and collagen production with a ratio of sGAG:collagen similar to that of native AF tissue. Moreover, it could be observed that several collagen fibers were arranged in regularly aligned bundles in the designed pore channels. Only when the fibrin seeding method was

used, the phenotype of the differentiated hASCs was similar to that of native AF cells. In conclusion, fibrin gel seeding of hASCs in an AF-mimetic PTMC scaffold and subsequent culturing in the presence of TGF-β3 is a strategy with great potential to engineer AF tissue *in vitro*.

Acknowledgement

This work was funded by the AO foundation and Academy of Finland. In addition, we would like to acknowledge Dr. Zhen Li, Dr. Sibylle Grad, Dr. David Eglin and Prof. Dr. Mauro Alini of the AO Research Institute for contributions to this work.

References

Ameer, G.A., Mahmood, T.A., Langer, R., 2002. A biodegradable composite scaffold for cell transplantation. Journal of Orthopaedic Research 20 (1), 16-19.

Bao, Q.B., Mccullen, G.M., Higham, P.A., Dumbleton, J.H., Yuan, H.A., 1996. The artificial disc: Theory, design and materials. Biomaterials 17 (12), 1157-67.

Bhattacharjee, M., Miot, S., Gorecka, A., Singha, K., Loparic, M., Dickinson, S., Das, A., Bhavesh, N.S., Ray, A.R., Martin, I., Ghosh, S., 2012. Oriented lamellar silk fibrous scaffolds to drive cartilage matrix orientation: Towards annulus fibrosus tissue engineering. Acta biomaterialia 8 (9), 3313-25.

Bibby, S.R., Jones, D.A., Lee, R.B., Yu, J., Urban, J.P.G., 2001. The pathophysiology of the intervertebral disc. Joint Bone Spine 68 (6), 537-42.

Bieback, K., Hecker, A., Schlechter, T., Hofmann, I., Brousos, N., Redmer, T., Besser, D., Kluter, H., Muller, A.M., Becker, M., 2012. Replicative aging and differentiation potential of human adipose tissue-derived mesenchymal stromal cells expanded in pooled human or fetal bovine serum. Cytotherapy 14 (5), 570-583.

Blanquer, S.B.G., Grijpma, D.W., Poot, A.A., 2015. Delivery systems for the treatment of degenerated intervertebral discs. Advanced Drug Delivery Reviews 84, 172-187.

Blanquer, S.B.G., Haimi, S.P., Poot, A.A., Grijpma, D.W., 2013. Effect of pore characteristics on mechanical properties and annulus fibrosus cell seeding and proliferation in designed ptmc tissue engineering scaffolds. Macromol. Symp. 334, 75–81.

Bron, J.L., Helder, M.N., Meisel, H.J., Van Royen, B.J., Smit, T.H., 2009. Repair, regenerative and supportive therapies of the annulus fibrosus: Achievements and challenges. Eur Spine J. 18 (3), 301-313.

Cassidy, J.J., Hiltner, A., Baer, E., 1989. Hierarchical structure of the intervertebral-disk. Connective Tissue Research 23 (1), 75-88.

Chou, Y.F., Zuk, P.A., Chang, T.L., Benhaim, P., Wu, B.M., 2011. Adipose-derived stem cells and bmp2: Part 1. Bmp2-treated adipose-derived stem cells do not improve repair of segmental femoral defects. Connective Tissue Research 52 (2), 109-118.

Clouet, J., Grimandi, G., Pot-Vaucel, M., Masson, M., Fellah, H.B., Guigand, L., Cherel, Y., Bord, E., Rannou, F., Weiss, P., Guicheux, J., Vinatier, C., 2009. Identification of phenotypic discriminating markers for intervertebral disc cells and articular chondrocytes. Rheumatology 48 (11), 1447-1450.

Colombini, A., Lopa, S., Ceriani, C., Lovati, A.B., Croiset, S.J., Di Giancamillo, A., Lombardi, G., Banfi, G., Moretti, M., 2014. In vitro characterization and in vivo behavior of human nucleus pulposus and annulus fibrosus cells in clinical-grade fibrin and collagen-enriched fibrin gels. Tissue Eng Part A DOI: 10.1089/ten.tea.2014.0279.

Coppes, M.H., Marani, E., Thomeer, R.T.W.M., Oudega, M., 1990. Innervation of annulus fibrosis in low-back-pain. Lancet 336 (8708), 189-190.

De Mulder, E.L.W., Hannink, G., Verdonschot, N., Buma, P., 2013. Effect of polyurethane scaffold architecture on ingrowth speed and collagen orientation in a subcutaneous rat pocket model. Biomedical Materials 8 (2).

Disch, A.C., Schmoelz, W., Matziolis, G., Schneider, S.V., Knop, C., Putzier, M., 2008. Higher risk of adjacent segment degeneration after floating fusions: Long-term outcome after low lumbar spine fusions. Journal of Spinal Disorders & Techniques 21 (2), 79-85.

Dominici, M., Le Blanc, K., Mueller, I., Slaper-Cortenbach, I., Marini, F., Krause, D., Deans, R., Keating, A., Prockop, D., Horwitz, E., 2006. Minimal criteria for defining multipotent mesenchymal stromal cells. The international society for cellular therapy position statement. Cytotherapy 8(4), 315-7.

Ebara, S., Iatridis, J.C., Setton, L.A., Foster, R.J., Mow, V.C., Weidenbaum, M., 1996. Tensile properties of nondegenerate human lumbar anulus fibrosus. Spine (Phila Pa 1976) 21 (4), 452-61.

Edwards, C.A., Obrien, W.D., 1980. Modified assay for determination of hydroxyproline in a tissue hydrolyzate. Clinica Chimica Acta 104 (2), 161-167.

Engelmayr, G.C., Papworth, G.D., Watkins, S.C., Mayer, J.E., Sacks, M.S., 2006. Guidance of engineered tissue collagen orientation by large-scale scaffold microstructures. Journal of Biomechanics 39 (10), 1819-1831.

Fazzalari, N.L., Costi, J.J., Hearn, T.C., Fraser, R.D., Vernon-Roberts, B., Hutchinson, J., Manthey, B.A., Parkinson, I.H., Sinclair, C., 2001. Mechanical and pathologic

consequences of induced concentric anular tears in an ovine model. Spine (Phila Pa 1976). 2001 Dec 1;26(23):2575-81.

Fink, T., Lund, P., Pilgaard, L., Rasmussen, J.G., Duroux, M., Zachar, V., 2008. Instability of standard pcr reference genes in adipose-derived stem cells during propagation, differentiation and hypoxic exposure. Bmc Molecular Biology 9.

Gabrielsson, B.G., Olofsson, L.E., Sjogren, A., Jernas, M., Elander, A., Lonn, M., Rudemo, M., Carlsson, L.M.S., 2005. Evaluation of reference genes for studies of gene expression in human adipose tissue. Obesity Research 13 (4), 649-652.

Gruber, H.E., Deepe, R., Hoelscher, G.L., Ingram, J.A., Norton, H.J., Scannell, B., Loeffler, B.J., Zinchenko, N., Hanley, E.N., Tapp, H., 2010. Human adipose-derived mesenchymal stem cells: Direction to a phenotype sharing similarities with the disc, gene expression profiling, and coculture with human annulus cells. Tissue Eng 16(9), 2843-60.

Gruber, H.E., Hoelscher, G., Ingram, J.A., Hanley, E.N., 2009. Culture of human anulus fibrosus cells on polyamide nanofibers extracellular matrix production. Spine 34 (1), 4-9.

Gruber, H.E., Ingram, J.A., Norton, H.J., Hanley, E.N., 2007. Senescence in cells of the aging and degenerating intervertebral disc - immunolocalization of senescence-associated beta-galactosidase in human and sand rat discs. Spine 32 (3), 321-327.

Guillaume, O., Daly, A., Lennon, K., Gansau, J., Buckley, S.F., Buckley, C.T., 2014. Shape-memory porous alginate scaffolds for regeneration of the annulus fibrosus: Effect of tgf-beta 3 supplementation and oxygen culture conditions. Acta Biomaterialia 10 (5), 1985-1995.

Guterl, C.C., See, E.Y., Blanquer, S.B.G., Pandit, A., Ferguson, S.J., Benneker, L.M., Grijpma, D.W., Sakai, D., Eglin, D., Alini, M., Iatridis, J.C., Grad, S., 2013. Challenges and strategies in the repair of ruptured annulus fibrosus. European Cells & Materials 25, 1-21.

Haimi, S., Moimas, L., Pirhonen, E., Lindroos, B., Huhtala, H., Raty, S., Kuokkanen, H., Sandor, G.K., Miettinen, S., Suuronen, R., 2009a. Calcium phosphate surface treatment of bioactive glass causes a delay in early osteogenic differentiation of adipose stem cells. J Biomed Mater Res A 91 (2), 540-7.

Haimi, S., Suuriniemi, N., Haaparanta, A.M., Ella, V., Lindroos, B., Huhtala, H., Raty, S., Kuokkanen, H., Sandor, G.K., Kellomaki, M., Miettinen, S., Suuronen, R., 2009b. Growth and osteogenic differentiation of adipose stem cells on pla/bioactive glass and pla/beta-tcp scaffolds. Tissue Engineering Part A 15 (7), 1473-1480.

Haschtmann, D., Ferguson, S.J., Stoyanov, J.V., 2012. Bmp-2 and tgf-beta3 do not prevent spontaneous degeneration in rabbit disc explants but induce ossification of the annulus fibrosus. European spine journal : official publication of the European

Spine Society, the European Spinal Deformity Society, and the European Section of the Cervical Spine Research Society 21 (9), 1724-33.

Hegewald, A.A., Cluzel, J., Kruger, J.P., Endres, M., Kaps, C., Thome, C., 2014. Effects of initial boost with tgf-beta 1 and grade of intervertebral disc degeneration on 3d culture of human annulus fibrosus cells. Journal of orthopaedic surgery and research 9, 73.

Jenner, J.M., Van Eijk, F., Saris, D.B., Willems, W.J., Dhert, W.J., Creemers, L.B., 2007. Effect of transforming growth factor-beta and growth differentiation factor-5 on proliferation and matrix production by human bone marrow stromal cells cultured on braided poly lactic-co-glycolic acid scaffolds for ligament tissue engineering. Tissue engineering 13 (7), 1573-82.

Kuh, S.U., Zhu, Y.R., Li, J., Tsai, K.J., Fei, Q.M., Hutton, W.C., Yoon, T.S., 2009. A comparison of three cell types as potential candidates for intervertebral disc therapy: Annulus fibrosus cells, chondrocytes, and bone marrow derived cells. Joint Bone Spine 76 (1), 70-74.

Kyllonen, L., Haimi, S., Mannerstrom, B., Huhtala, H., Rajala, K.M., Skottman, H., Sandor, G.K., Miettinen, S., 2013. Effects of different serum conditions on osteogenic differentiation of human adipose stem cells in vitro. Stem Cell Research & Therapy 4.

Lee, C.R., Grad, S., Gorna, K., Gogolewski, S., Goessl, A., Alini, M., 2005. Fibrin-polyurethane composites for articular cartilage tissue engineering: A preliminary analysis. Tissue Engineering 11 (9-10), 1562-1573.

Lindroos, B., Suuronen, R., Miettinen, S., 2011. The potential of adipose stem cells in regenerative medicine. Stem Cell Reviews and Reports 7 (2), 269-291.

Marchand, F., Ahmed, A.M., 1990. Investigation of the laminate structure of lumbar disc anulus fibrosus. Spine (Phila Pa 1976) 15 (5), 402-10.

Melchels, F.P.W., Feijen, J., Grijpma, D.W., 2010. A review on stereolithography and its applications in biomedical engineering. Biomaterials 31 (24), 6121-6130.

Mwale, F., Roughley, P., Antoniou, J., 2004 Distinction between the extracellular matrix of the nucleus pulposus and hyaline cartilage: A requisute for tissue engineering of intervertebral disc European Cells & Materials 8, 58-64.

Nerurkar, N.L., Baker, B.M., Sen, S., Wible, E.E., Elliott, D.M., Mauck, R.L., 2009. Nanofibrous biologic laminates replicate the form and function of the annulus fibrosus. Nature Materials 8 (12), 986-992.

Nerurkar, N.L., Elliott, D.M., Mauck, R.L., 2010. Mechanical design criteria for intervertebral disc tissue engineering. Journal of Biomechanics 43 (6), 1017-1030.

Nesti, L.J., Li, W.J., Shanti, R.M., Jiang, Y.J., Jackson, W., Freedman, B.A., Kuklo, T.R., Giuliani, J.R., Tuan, R.S., 2008. Intervertebral disc tissue engineering using a novel hyaluronic acid-nanofibrous scaffold (hanfs) amalgam. Tissue Eng Part A 14 (9), 1527-37.

Orozco, L., Soler, R., Morera, C., Alberca, M., Sanchez, A., Garcia-Sancho, J., 2011. Intervertebral disc repair by autologous mesenchymal bone marrow cells: A pilot study. Transplantation 92 (7), 822-828.

Park, S.H., Gil, E.S., Mandal, B.B., Cho, H., Kluge, J.A., Min, B.H., Kaplan, D.L., 2012. Annulus fibrosus tissue engineering using lamellar silk scaffolds. Journal of tissue engineering and regenerative medicine 6 Suppl 3, s24-33.

Perie, D., Korda, D., Iatridis, J.C., 2005. Confined compression experiments on bovine nucleus pulposus and annulus fibrosus: Sensitivity of the experiment in the determination of compressive modulus and hydraulic permeability. Journal of Biomechanics 38 (11), 2164-2171.

Pfaffl, M.W., 2001. A new mathematical model for relative quantification in real-time rt-pcr. Nucleic Acids Research 29 (9).

Richardson, S.M., Hoyland, J.A., Mobasheri, R., Csaki, C., Shakibaei, M., Mobasheri, A., 2010. Mesenchymal stem cells in regenerative medicine: Opportunities and challenges for articular cartilage and intervertebral disc tissue engineering. Journal of Cellular Physiology 222 (1), 23-32.

Roughley, P., Martens, D., Rantakokko, J., Alini, M., Mwale, F., Antoniou, J., 2006. The involvement of aggrecan polymorphism in degeneration of human intervertebral disc and articular cartilage. Eur Cell Mater 11, 1-7.

Roughley, P.J., 2004. Biology of intervertebral disc aging and degeneration - involvement of the extracellular matrix. Spine 29 (23), 2691-2699.

Schuller-Ravoo, S., Teixeira, S.M., Feijen, J., Grijpma, D.W., Poot, A.A., 2013. Flexible and elastic scaffolds for cartilage tissue engineering prepared by stereolithography using poly(trimethylene carbonate)-based resins. Macromolecular Bioscience 13 (12), 1711-1719.

Sha'ban, M., Yoon, S.J., Ko, Y.K., Ha, H.J., Kim, S.H., So, J.W., Idrus, R.B., Khang, G., 2008. Fibrin promotes proliferation and matrix production of intervertebral disc cells cultured in three-dimensional poly(lactic-co-glycolic acid) scaffold. J Biomater Sci Polym Ed 19 (9), 1219-37.

Skoog, S.A., Goering, P.L., Narayan, R.J., 2014. Stereolithography in tissue engineering. Journal of Materials Science-Materials in Medicine 25 (3), 845-856.

Tapp, H., Deepe, R., Ingram, J.A., Kuremsky, M., Hanley, E.N., Jr., Gruber, H.E., 2008. Adipose-derived mesenchymal stem cells from the sand rat: Transforming growth

factor beta and 3d co-culture with human disc cells stimulate proteoglycan and collagen type i rich extracellular matrix. Arthritis Res Ther. 10(4), R89.

Turner, K.G., Ahmed, N., Santerre, J.P., Kandel, R.A., 2014. Modulation of annulus fibrosus cell alignment and function on oriented nanofibrous polyurethane scaffolds under tension. Spine Journal 14 (3), 424-434.

Vyner, M.C., Li, A.N., Amsden, B.G., 2014. The effect of poly(trimethylene carbonate) molecular weight on macrophage behavior and enzyme adsorption and conformation. Biomaterials 35 (33), 9041-9048.

Wipff, P.J., Hinz, B., 2008. Integrins and the activation of latent transforming growth factor beta1 - an intimate relationship. European journal of cell biology 87 (8-9), 601-15.

Zhang, Z., Kuijer, R., Bulstra, S.K., Grijpma, D.W., Feijen, J., 2006. The in vivo and in vitro degradation behavior of poly(trimethylene carbonate). Biomaterials 27 (9), 1741-1748.

Table 1: Medium compositions used in the study

Medium	*Composition*
Maintenance medium (MM)	DMEM-F12 (Gibco); 5-10% human serum (PAA Laboratories GmbH, Austria); 1% antibiotics (100 U/ml penicillin; 100 µg/ml streptomycin; Lonza Biowhittaker, Belgium); 1% vol L-alanyl-L-glutamine (Glutamax I, Gibco)
Control chondogenic medium (CM)	DMEM-F12(Gibco®); ITS+1 (BD Biosciences); 0.3% vol antibiotics (100 U/ml penicillin; 100 µg/ml streptomycin; Lonza); 1% vol L-alanyl-L-glutamine (Glutamax I; Gibco®); 50 µg/ml L-Ascorbic acid 2-phosphate (Sigma-Aldrich, Munich, Germany); 55 µg/ml sodium pyruvate (Lonza); 23 µg/ml L-proline (Sigma-Aldrich)
DM1	CM containing 10 ng/ml TGF-β1 (Santa Cruz, Dallas, TX, USA)
DM3	CM containing 10 ng/ml TGF-β3 (Prospec, Rehovot, Israel)
DM1+3	CM containing 10 ng/ml TGF-β1, 10 ng/ml TGF-β3

Table 2: Reverse and forward primer sequences used for PCR assay

Gene	Primer sequence		Product size
acidic ribosomal phosphoprotein P0	Forward:	5'-AAT CTC CAG GGG CAC CAT T-3'	70 bp
	Reverse	5'-CGC TGG CTC CCA CTT TGT-3'	
aggrecan	Forward:	5'-TCG AGG ACA GCG AGG CC-3'	85 bp
	Reverse:	5'-TCG AGG GTG TAG CGT GTA GAG A-3'	
decorin	Forward:	5’- CTC TGC TGT TGA CAA TGG CTC TCT -3’	135 bp
	Reverse:	5’- TGG ATG GCT GTA TCT CCC AGT ACT -3’	
collagen type I	Forward:	5'-CCA GAA GAA CTG GTA CAT CAG CAA-3'	140 bp
	Reverse:	5'-CGC CAT ACT CGA ACT GGA ATC-3'	
collagen type II	Forward:	5'-GAG ACA GCA TGA CGC CGA G-3'	67 bp
	Reverse:	5'-GCG GAT GCT CTC AAT CTG GT-3'	
collagen type V	Forward:	5'-TGA GTT GTG GAG CTG ACT CTA ATC-3'	181 bp
	Reverse:	5'-TAA CAG AAG CAT AGC ACC TTT CAG-3'	

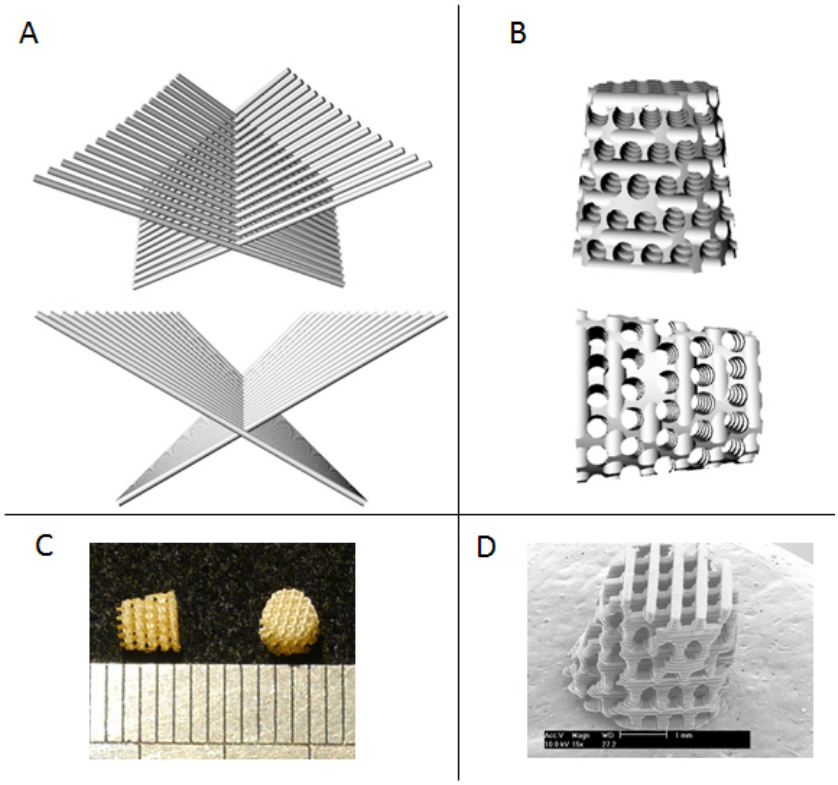

Figure 1: Computer-aided design (CAD) representation of 15 bilayer lamella of collagen (A) with the typical overlapping lamella organization and angle-ply (from 30° to 45°) of the native AF. CAD representation of the the 3D scaffold,(B) with the pore channels that follow the orientation from peripheral to central as the collagen fibres in the native AF tissue. Photographic image of the PTMC scaffolds built by stereolithography (C). High resolution SEM image of the built PTMC scaffold (D).

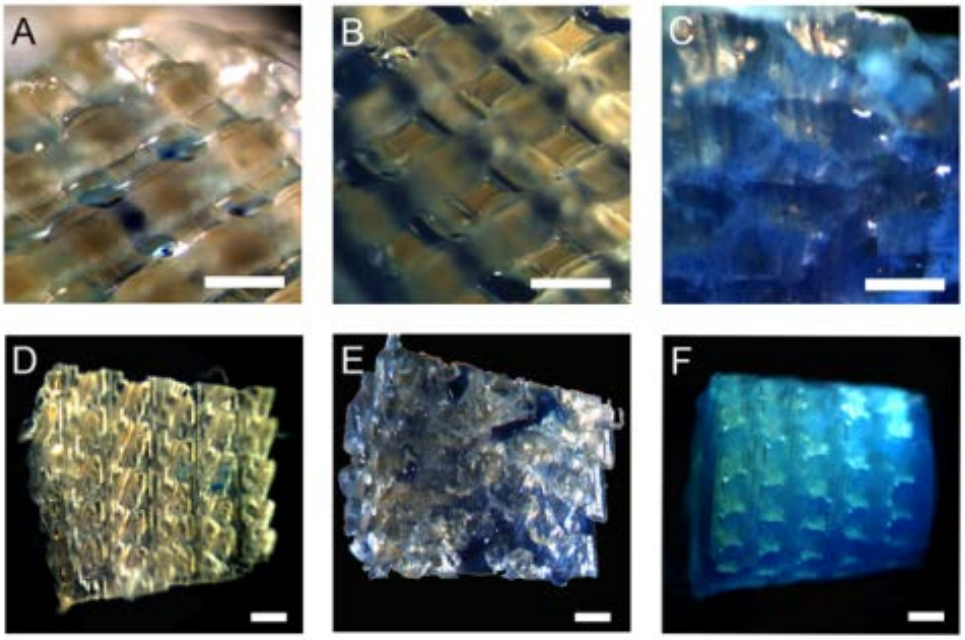

Figure 2: Methylene blue staining of differentiated hASCs seeded with direct (A and D), micromass (B and E) and fibrin gel (C and F) techniques in scaffolds at 1 and 14 days. Scale bar: 500µm.

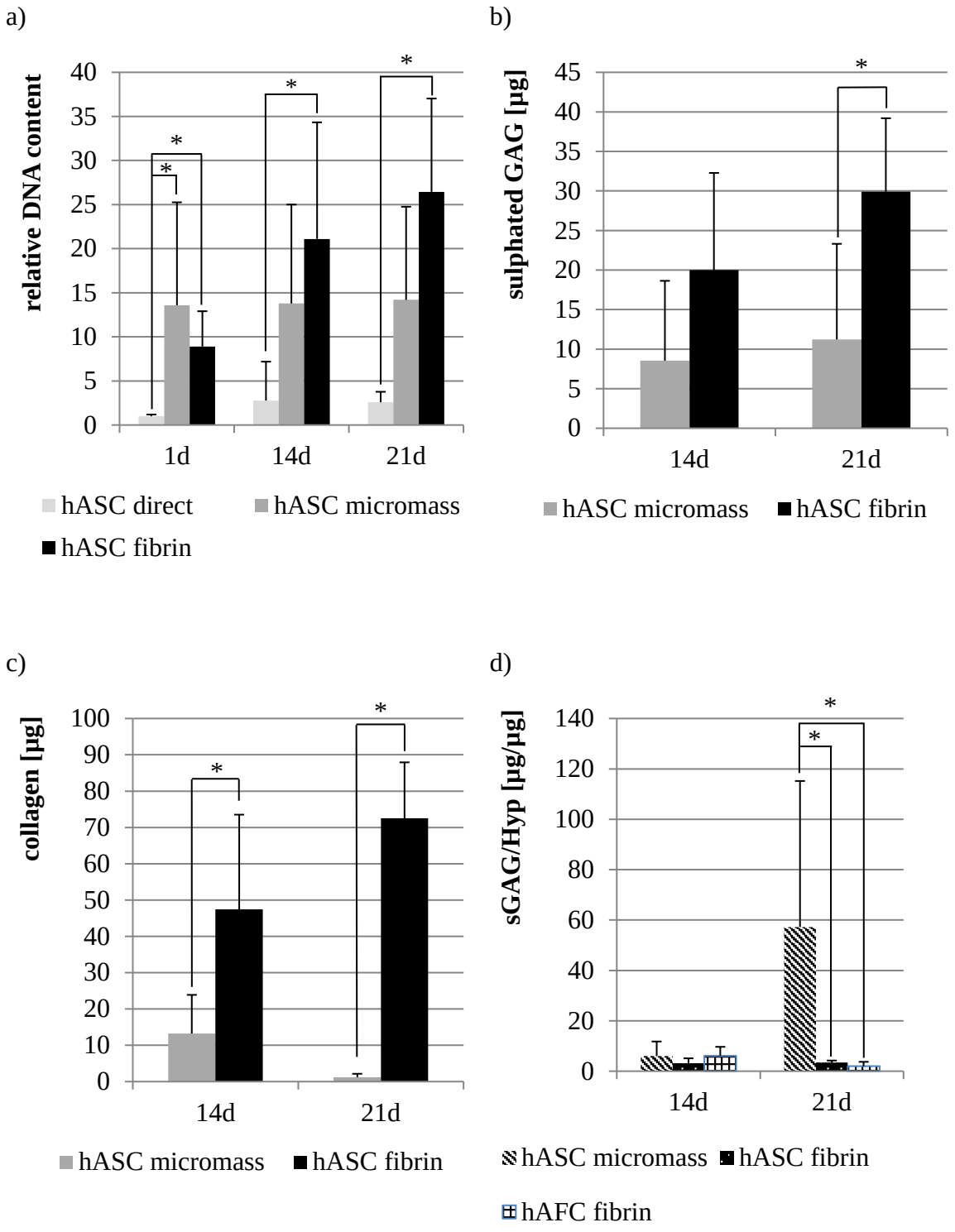

Figure 3: Relative DNA content of differentiated hASCs seeded with direct, micromass and fibrin seeding after 1, 14 and 21 days of culture (a); Sulphated GAG content (b) and total collagen (c) of differentiated hASCs seeded with micromass and fibrin seeding at 14 and 21 days of culture. Sulphated GAG/hydroxyproline ratio

(d) of differentiated hASCs seeded with micromass and fibrin seeding and human AF cells at 14 and 21 days of culture. The results are expressed as mean ± standard deviation (* $p<0.05$).

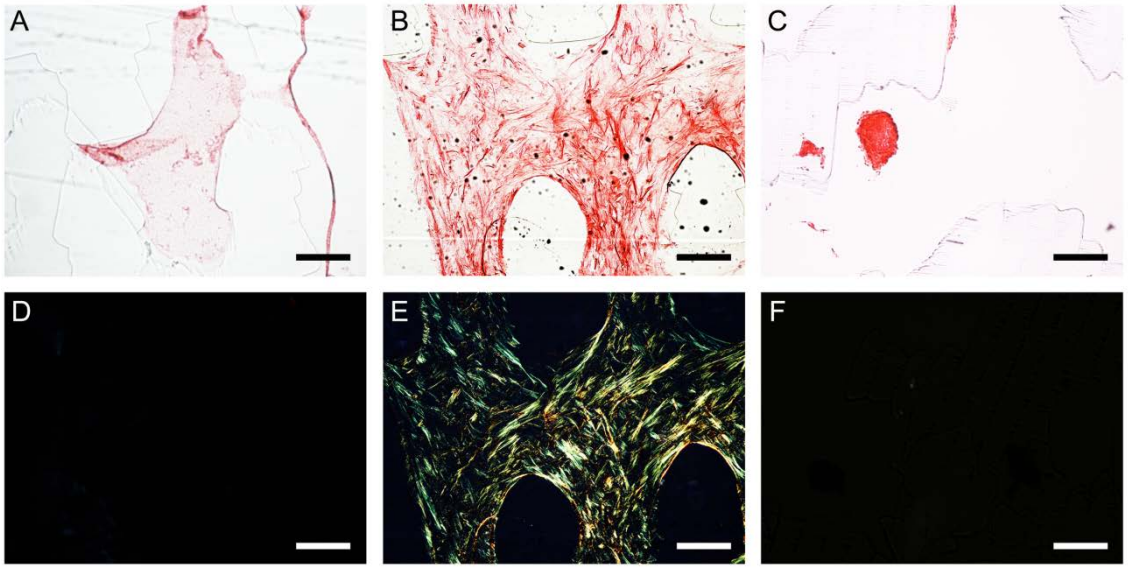

Figure 4: Picrosirius red staining of collagen and deposition of collagen fiber bundles (polarized light shows the alignment of collagen fibres) of differentiated hASCs using fibrin gel (B and E) and micromass (C and F) seeding at 21 day time point as well as the blank scaffold with fibrin without cell (A and D) . Scale bar: 200 µm

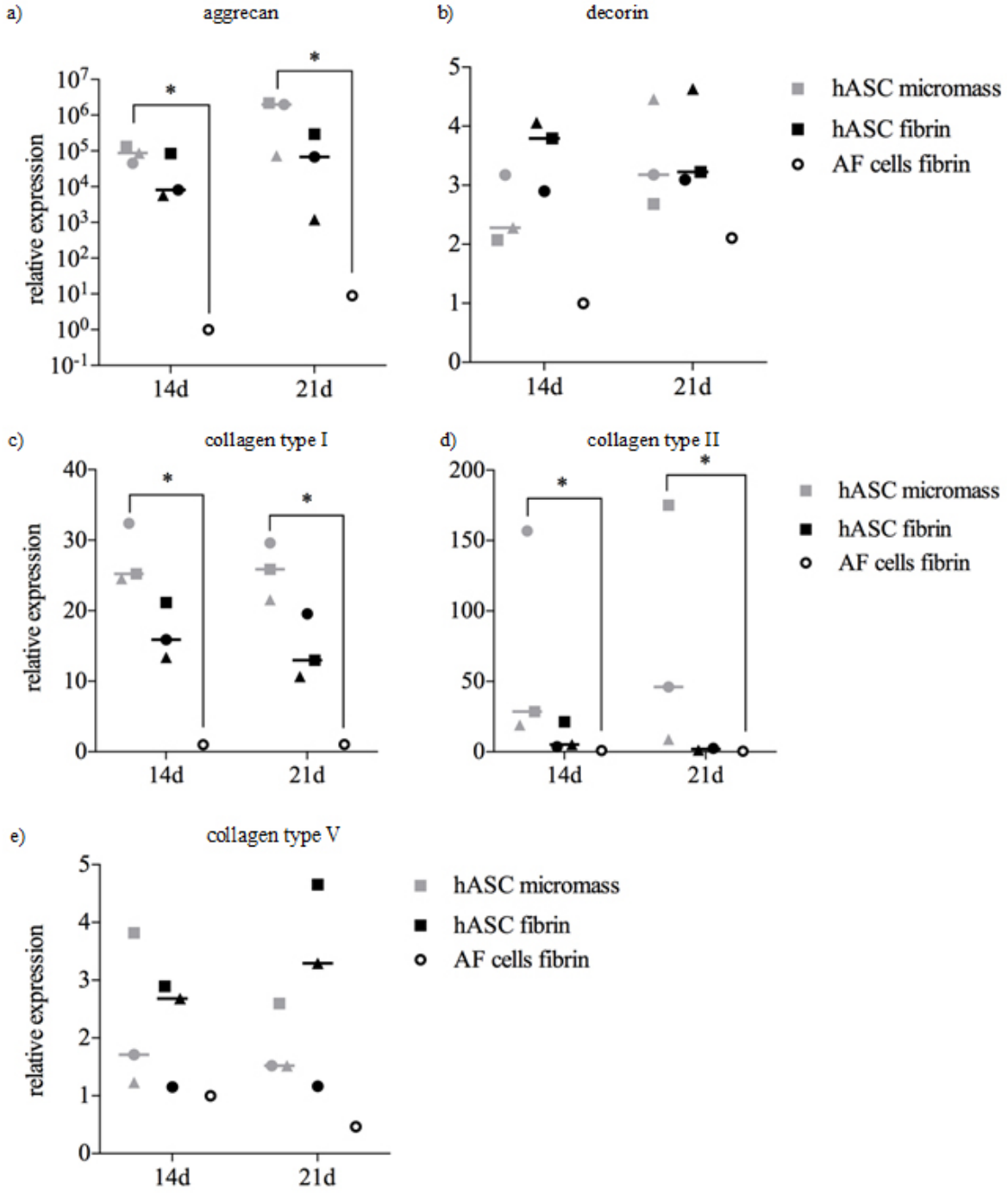

Figure 5: The relative expression of aggrecan (a), decorin (b), collagen type I (c), collagen type II (d) and collagen type V (e) of differentiated hASC and human AF cells seeded scaffolds at 14 and 21 days of culture. The results are presented relative to the mean expression in human AF cells at 14 days. The different markers in the figure indicate different donors. Median expression is marked with a horizontal line (* $p<0.05$).

a)

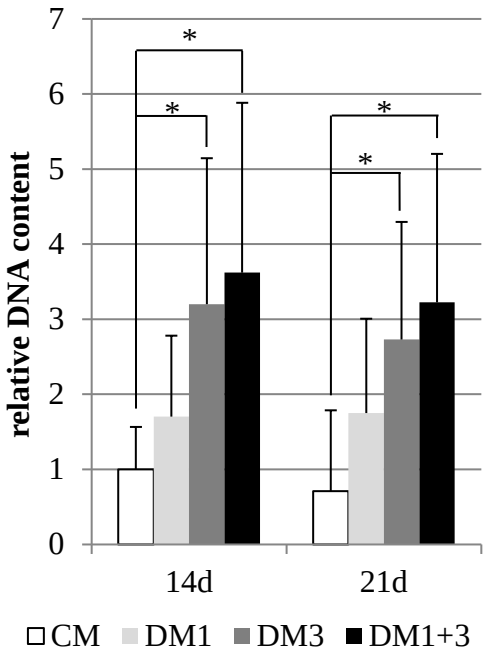
relative DNA content
7
6
5
4
3
2
1
0
*
*
*
*
14d
21d
CM
DM1
DM3
DM1+3

b)

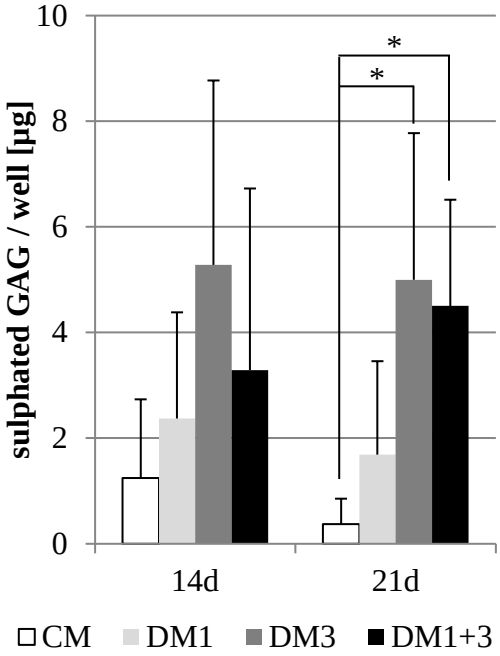
sulphated GAG / well [µg]
10
8
6
4
2
0
*
*
14d
21d
CM
DM1
DM3
DM1+3

c)

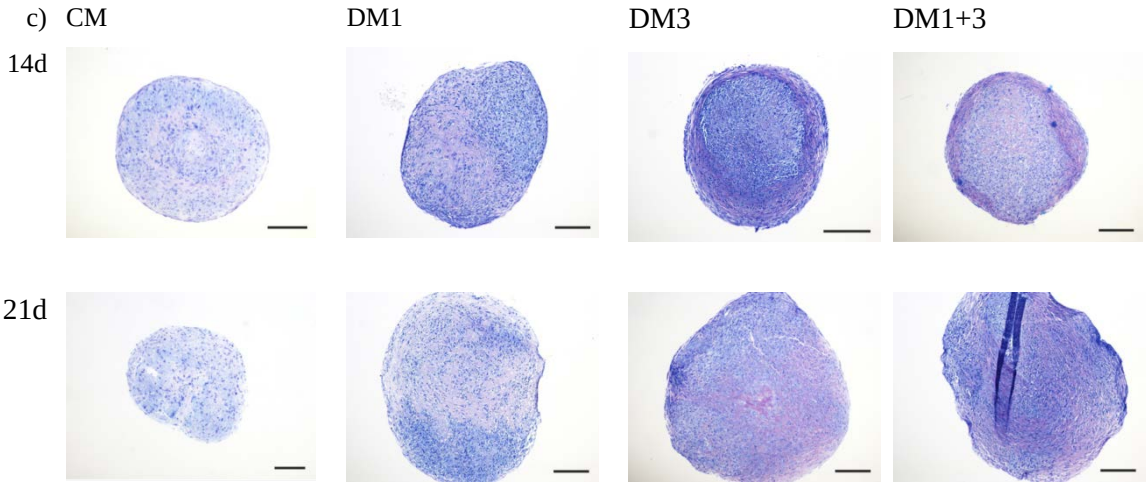
CM
DM1
DM3
DM1+3
14d
21d

d)

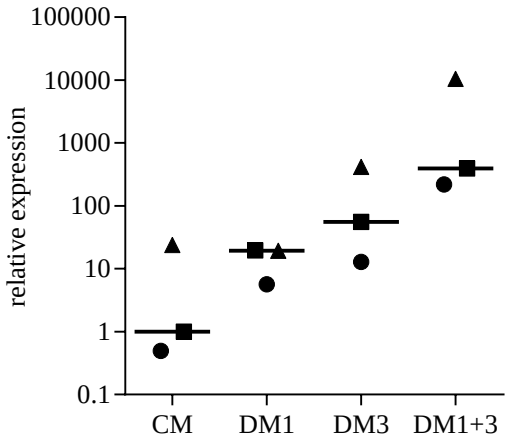

Supplementary figure 1: a) DNA content, b) sulphated GAG content c) Toluidine blue staining; nucleic acids are stained blue and proteoglycans and their associated GAGs are stained purple (Scale bar: 500µm) d) aggregan gene expression of hASC micromasses cultured for 14 and 21 days in chondrogenic medium (CM), CM supplemented with 10 ng/ml TGFβ1 (DM1), 10 ng/ml TGF-β3 (DM3) or both 10 ng/ml TGFβ1 and 10 ng/ml TGFβ (DM1+3). The results are expressed as mean ± standard deviation (* $p<0.05$). Based on these results DM3 was selected for the further experiments.

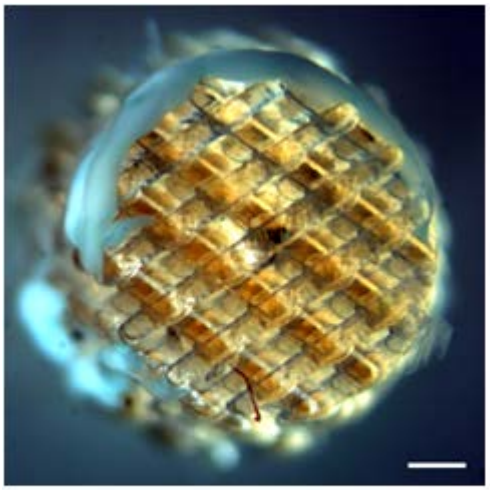

Supplementary figure 2: Methylene blue-stained scaffold with fibrin and without hASCs, demonstrating that fibrin gel alone did not take up significantly the methylene blue dye.